MULTIPOLE CHARACTER OF THE LARGE-AMPLITUDE, LOW FREQUENCY RESONANCES IN THE SONAR ECHOES OF SUBMERGED SPHERICAL SHELLS

HANS C. STRIFORS

National Defense Research Establishment (FOA 2), S-172 90 Sundbyberg, Sweden

and

GUILLERMO C. GAUNAURD

Naval Surface Warfare Center, Research Department (Code R-42), Silver Spring,
MD 20903-5000, U.S.A.

Abstract — We analyze the large-amplitude resonance features, which are present at low frequencies in the backscattering cross-sections (BSCS) of air-filled, spherical, elastic shells submerged in water. By means of partial-wave expansions we demonstrate the multipole character of those features. For the materials and thicknesses investigated, it is confirmed that about half-a-dozen modes contribute to their formation. As the shell thickness decreases we note that: (i) fewer modes are seen to contribute to the BSCS. Ultimately, as the shell thickness approaches zero, only the monopole, $n = 0$, mode has an effect, just as for an air-bubble in water. (ii) In the bubble case, the large amplitude becomes *giant*, the various peaks coalesce into one, and its spectral location shifts down to $k_1 a \sim 10^{-3}$. (iii) The narrow, low-amplitude set of overtones caused by the internal air remains present at all thicknesses, as the shell thickness decreases. Finally, we give a physical interpretation for these large features. They seem to be caused by a pseudo-Lamb wave denoted here by a_0^1, investigated earlier by Junger (1967), by means of Donnell's shell theory. This wave is slower than the generalized zeroth-order antisymmetric a_0, Lamb wave for a shell. Its dispersion plot —which we display —exists only in the same narrow, low-frequency spectral band where the large echo features in question also occur. We investigate here its cause and effect by means of an exact, three-dimensional elasticity description of the shell motions, which was derived earlier by Ayres *et al.* (1987). We emphasize that what we have called, here and in the referenced paper, the a_0-wave, is really a "generalized" antisymmetric zeroth-order Lamb wave for a *shell*, fluid-loaded on both sides by dissimilar fluids (and not for a *plate* in *vacuum*, as is often done). The a_0^1-wave is a companion type of generalized a_0-wave for shells that emerges from the roots of the same characteristic equation, and which has no counterpart for flat plates.

I. INTRODUCTION

Perhaps the most noticeable and dominant of all features present in the backscattered echo from an air-filled, spherical elastic shell in water, at low frequencies, is a large resonance that appears in the Rayleigh region (viz. $a/\lambda < 1$, a being the outer radius of the shell and λ the wavelength in water). For a metal shell in water, the pressure amplitude of this echo feature is ≈ 10 dB above the background it is superimposed on. Analyzing the low-frequency response of shells as manifested in the echoes they return to a distant sensor, it is clear that this feature is so prominent that it will be the first one detected, and the easiest to use as a target-classifier by an active sonar operating at low frequencies. At first sight, this feature appears to be a single spike, like in an air-bubble in water, but closer inspection shows that it is composed of several peaks. They seem to be caused by several multipole components. We will show below that this is indeed the case. We study this feature using our earlier approach (Ayres *et al.*, 1987; Gaunaurd and Werby, 1987) in which the shell vibration was analyzed by means of the exact equations of three-dimensional elasticity. We compare our results with those obtained with an earlier approach based on shell theory. We give a physical interpretation for its origin, and display the dispersion curve of the a_0^1-wave that causes it. This is a relatively slow wave due to shell curvature that only exists in a narrow frequency band at the low end of the BSCS.

2. THEORETICAL BACKGROUND

A thin, air-filled, spherical elastic shell submerged in water has outer radius a and inner radius b. It is insonified at its South pole (defined by the spherical coordinate $\theta = \pi$) by a plane sound wave that emerges from a disant source. Its normalized backscattering cross-section σ is given by (cf., i.e. Ayres et al., 1987):

$$\frac{\sigma}{\pi a^2} = |f_\infty (\pi, x)|^2 = \left| \sum_{n=0}^{\infty} f_n(\pi, x) \right|^2 = \left| \frac{2}{ix} \sum_{n=0}^{\infty} (-1)^n (2n+1) A_n(x) \right|^2 . \tag{1}$$

where $f_\infty (\pi, x)$ is the form-function in the backscattering direction $\theta = \pi$. Here $x \equiv k_1 a$, where $k_1 = \omega/c_1$ is the wave number. The circular frequency is ω and c_1 is the sound speed in the outer medium (i.e. medium No. 1, the water). The shell is medium No. 2, and the inner air is medium No. 3.

For each value of n the coefficients $A_n(x)$ are determined from the six boundary conditions at the interfaces $r = a, b$ (viz. continuity of radial displacement and normal stress, and vanishing shear stress) as ratios of two 6×6 determinants:

$$A_n(x) \equiv
\begin{vmatrix}
A_1^* & d_{12} & d_{13} & d_{14} & d_{15} & 0 \\
A_2^* & d_{22} & d_{23} & d_{24} & d_{25} & 0 \\
0 & d_{32} & d_{33} & d_{34} & d_{35} & 0 \\
0 & d_{42} & d_{43} & d_{44} & d_{45} & d_{46} \\
0 & d_{52} & d_{53} & d_{54} & d_{55} & d_{56} \\
0 & d_{62} & d_{63} & d_{64} & d_{65} & 0
\end{vmatrix}
\bigg/
\begin{vmatrix}
d_{11} & d_{12} & d_{13} & d_{14} & d_{15} & 0 \\
d_{21} & d_{22} & d_{23} & d_{24} & d_{25} & 0 \\
0 & d_{32} & d_{33} & d_{34} & d_{35} & 0 \\
0 & d_{42} & d_{43} & d_{44} & d_{45} & d_{46} \\
0 & d_{52} & d_{53} & d_{54} & d_{55} & d_{56} \\
0 & d_{62} & d_{63} & d_{64} & d_{65} & 0
\end{vmatrix} . \tag{2}$$

where the 30 non-vanishing elements d_{ij} and A_1^*, A_2^* have been listed in Ayres et al. (1987). It should be noted that the shell deformations are governed by the three-dimensional theory of elasticity, and no approximate shell theory has been introduced.

The elements of the determinants in eqn (2) all depend on x, $x_{d2} \equiv \omega/c_{d2}$, $x_{s2} \equiv \omega/c_{s2}$, and $x_3 \equiv \omega/c_3$, where c_{d2} (c_{s2}) is the dilatational (shear) wave speed in the shell, and c_3 is the sound speed in the inner air. Since these quantities can be expressed in terms of x, we indicate this dependence by $A_n(x)$. We note that eqns (1) and (2) for the backscattering cross-section and the modulus of the form-function (viz. $|f_\infty (\pi, x)|$) obtained for elastic materials can be conveniently generalized to viscoelastic materials using the methodology described by Strifors and Gaunaurd (1989). For viscoelastic materials complex-valued wave numbers replace the real-valued ones for elastic materials.

The modulus of the form-function has been plotted versus x in very broad frequency bands by Ayres et al. (1987) and Gaunaurd and Werby (1987). The partial waves $|f_n(\pi, x)|$, for $n = 0, 1, 2, \ldots$, defined in eqn (1) are the "normal modes" that make up the form-function, $|f_\infty (\pi, x)|$. In the very broad bands in which the form-functions have been previously displayed in the referenced papers, the low-frequency behavior is not clearly discernible, and it has received relatively little attention.

3. THE LOW-FREQUENCY BEHAVIOR CENTRE

Submerged spherical shells insonified at very low frequencies, have form-functions that exhibit noticeable resonance features in the (non-dimensional) frequency band: $0 < x < 4$. These features are of relatively large amplitudes and, at first sight, resemble the so-called giant monopole resonance (Gaunaurd et al., 1979) of air-bubbles in water. Since most of the past attention has been directed to the overall broadband spectral behavior, particularly at high frequencies, this large resonance has not yet received much study. Furthermore, in many earlier calculations pertaining to the cross-sections of elastic shells in water, the shells have been assumed evacuated. This assumption does not introduce significant errors in the

Table 1. Material properties of interest

Material	ρ (kg m^{-3})	$c_d(c)$ (m s^{-1})	c_t (m s^{-1})
Steel	7800	5880	3140
Water	1000	1500	—
Air	1.20	340	—

overall behavior, but as we will see below, it results in the neglect of certain narrow resonance families that are precisely due to the presence of internal air.

We will study all the resonance features in the above mentioned frequency band, and will exhibit the real *multipole* nature of the large features, as well as confirm the presence of the narrow resonance families caused by inner air. Moreover, we will see that as the shell thickness is decreased the large resonances approach the monopole resonance of air-bubbles in water. This means that: (i) the multipole character progressively disappears, (ii) the amplitude becomes "giant", and (iii) the single mode that eventually is seen to cause it (i.e. the mode $n = 0$) produces a single resonance frequency that shifts to lower values. Furthermore, the narrow resonance families due to the inner air remain present and visible throughout the entire limiting process $b \to a$, as shown below.

We note that in the very thin-shell limit, $b \to a$, the shell material actually disappears. Medium No. 2 is absent, and only media No. 1 and No. 3 remain. The coefficients in eqn (2) then reduce, after considerable algebra, to:

$$A_n(x) = - \frac{\rho_1 x j_n'(x) j_n(x_3) - \rho_1 x_3 j_n'(x_3) j_n(x)}{\rho_1 x h_n^{(1)'}(x) j_n(x_3) - \rho_1 x_3 j_n'(x_3) h_n^{(1)}(x)}, \tag{3}$$

where $j_n(\cdot)$ and $h_n^{(1)}(\cdot)$ denote the spherical Bessel function of the first kind of order n and the spherical Hankel function of the first kind of order n, respectively, and a prime denotes derivation with respect to the argument. Equation (3) is the exact expression of the coefficients for an air-bubble in water, cf. Gaunaurd *et al.* (1979). See also the recent review by Brill and Gaunaurd (1987), where this and various other limiting cases have been investigated. The right side of eqn (3) can be expressed exclusively in terms of x, since $x_3 = (c_1/c_3) \cdot x$ and c_1, c_3 are presumably known, as well as ρ_1, ρ_3. In the air-bubble case just mentioned, as well as in the limiting process for the progressively thinner metal shell of interest here, the RST (Resonance Scattering Theory) "background" (Brill and Gaunaurd, 1987) that must be suppressed to isolate the resulting resonances is the *soft* one, obtained from eqn (3) in the limit of a very tenuous (i.e. ultimately, evacuated) bubble of density $\rho_3/\rho_1 \to +0$. In this limit, the pertinent coefficients $A_n(x)$ to be used in eqn (1) reduce to:

$$A_n(x) = -j_n(x)/h_n^{(1)}(x). \tag{4}$$

4. NUMERICAL RESULTS AND DISCUSSION

The air-filled, steel shell in water and the acoustic media considered here have material properties of primary interest for wave propagation listed in Table 1. The wave speeds for steel have been computed using the values $E = 200$ GPa and $v = 0.3$ of Young's modulus and Poisson's ratio, respectively. The pertinent form-functions for this shell, of relative thicknesses: $h/a \equiv 1 - b/a = 2.5\%$, 1.0%, 0.1% and 0.01% are shown in Fig. 1, in the dimensionless frequency band: $0 \leqslant x \equiv k_1 a \leqslant 4$. In the upper plots we see that there are some large-amplitude resonance features occurring at frequencies between one and two-and-a-half. These amplitude peaks get to be as large as nine-and-a-half. In the lower plots, where the shell thicknesses are *very* small, we note that the multipole resonances have been replaced by a single one, which shifts down to smaller values of the frequency when the shell thickness is decreased. We also observe that the amplitude of the monopole resonance increases with decreasing shell thickness.
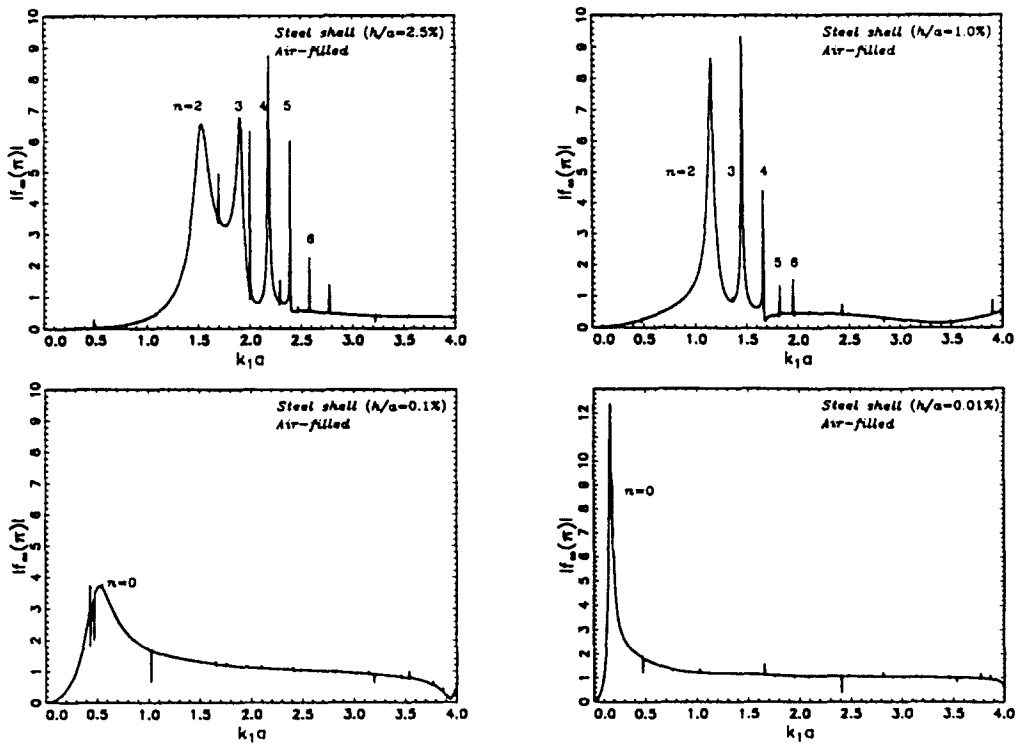
Fig. 1. Modulus of the form-function of an air-filled steel shell in water in the frequency range
$0 \leqslant k_1 a \leqslant 4$. Relative shell thickness $h/a = 2.5\%$, 1.0%, 0.1% and 0.01%.

In each plot in Fig. 1 there is also a low-amplitude narrow set of resonances that trails behind, and is superimposed on the "soft" background obtained by the coefficients in eqn (4). These narrow resonances are due to the inner air.

Next we examine the partial-waves $|f_n(\pi, x)|$ contained within the form-function (cf. eqn (1)). The first six of these normal modes (i.e. $n = 0, 1, \ldots, 5$) are plotted in Figs 2 and 3. Observation of Fig. 2 shows that each of the partial waves $n = 2, \ldots, 5$ contains a dominating resonance spike coincident with each of the main peaks present in the respective upper plot of Fig. 1. Thus, each of the resonance features in the form-function has its origin in each of the partial waves representing the modes, beginning with $n = 2$. It is not necessary to display partial-waves in Fig. 2 past $n = 5$ because the contribution to the presence of the resulting large feature for this material and thicknesses diminishes rapidly for larger values of n.

In Fig. 3 the corresponding plots of partial waves for the shells with relative thickness of only 0.1% and 0.01%. We see that the multipole resonances of Fig. 2 have disappeared while, instead, a monopole resonance $(n = 0)$ emerges. In the limit of vanishing shell thickness this monopole resonance approaches the giant resonance of an air-bubble that is displayed in Fig. 4. We have verified the limiting response numerically for a relative shell thickness as low as 10^{-8}. For the air-bubble in water the form-function is computed using the coefficients in eqn (3). It shows a main peak at $x \equiv k_1 a \approx 0.0136$ of magnitude $|f_0(\pi, x)| \approx 147$. This peak can be decomposed into a background portion and a residual or resonance portion in the usual manner of the RST as was shown by Gaunaurd et al. (1979), using a slightly different definition of form-function that accounts for the difference by a factor of two as compared with the value given here. The background is due to the bubble wall and shape, and the "resonance" is due to the internal air. Below the value $x \approx 0.01$ the curve exhibits a growth proportional to x^2 as predicted by the Rayleigh fourth-power law for scattering cross-sections, which are proportional to the square of the appropriate form-function. We note that the amplitude value 147 is about 22 dB above a background level of unity. Our exact bubble results agree well with approximate ones,
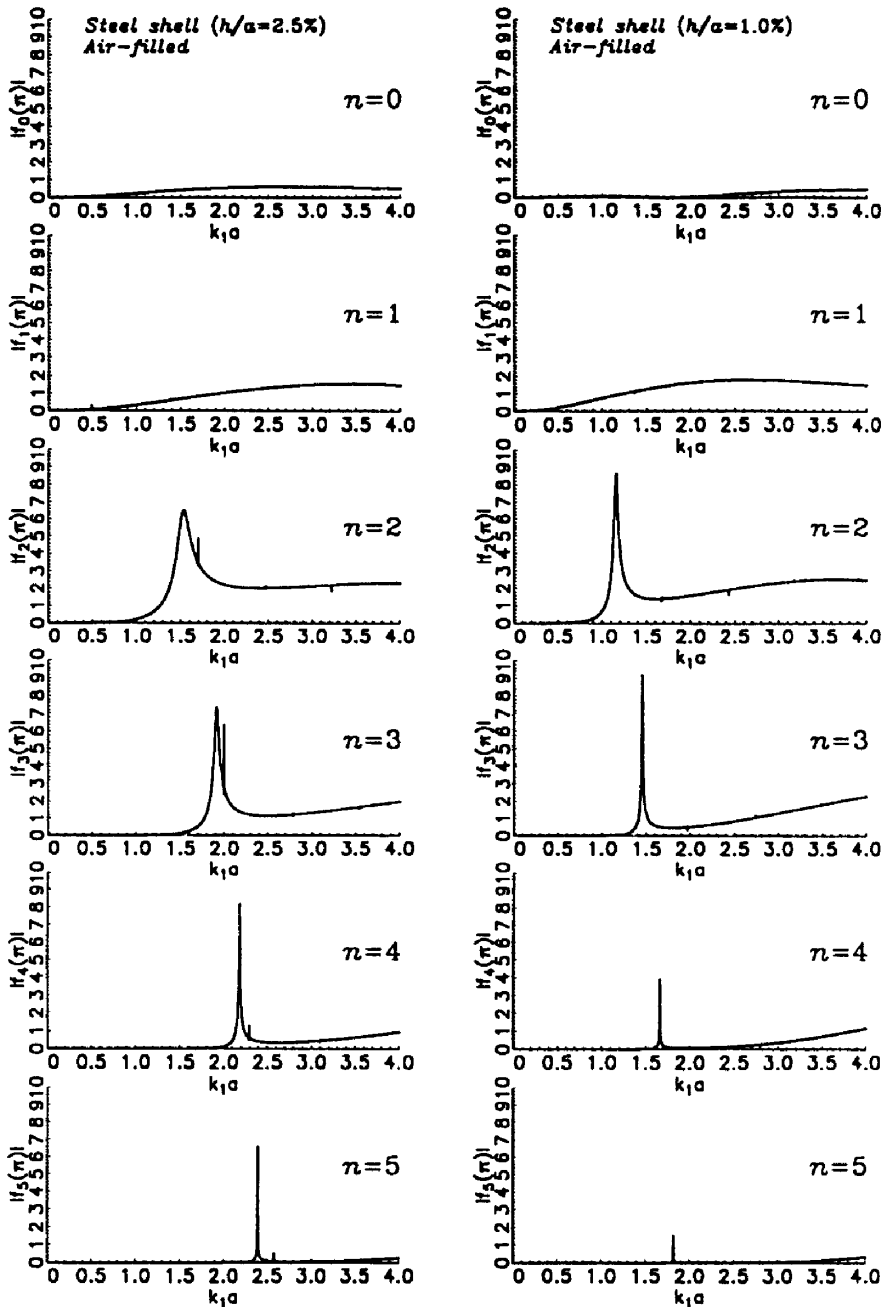
Fig. 2. The first few (n = 0, 1, ..., 5) partial waves contained within the backscattering cross-sections summed in the upper plots in Fig. 1. Relative shell thickness is 2.5% (1.0%) in the left (right) plots.

found in the early forties, which appeared in World War II Reports such as the much cited compendium edited by Major (1969).

5. PHYSICAL INTERPRETATION OF THE LARGE AMPLITUDE FEATURES

The large amplitude resonance features of shell cross-sections at low frequencies seem to be caused by a relatively slow shell wave that has a phase velocity lower than that of the a_0-wave (i.e. zeroth-order antisymmetric Lamb wave). We will denote this wave the "a_0^1-wave". It is closely related to the a_0-wave, since it emerges from an additional set of roots of the same characteristic equation. We call it a "shell wave", as opposed to a plate
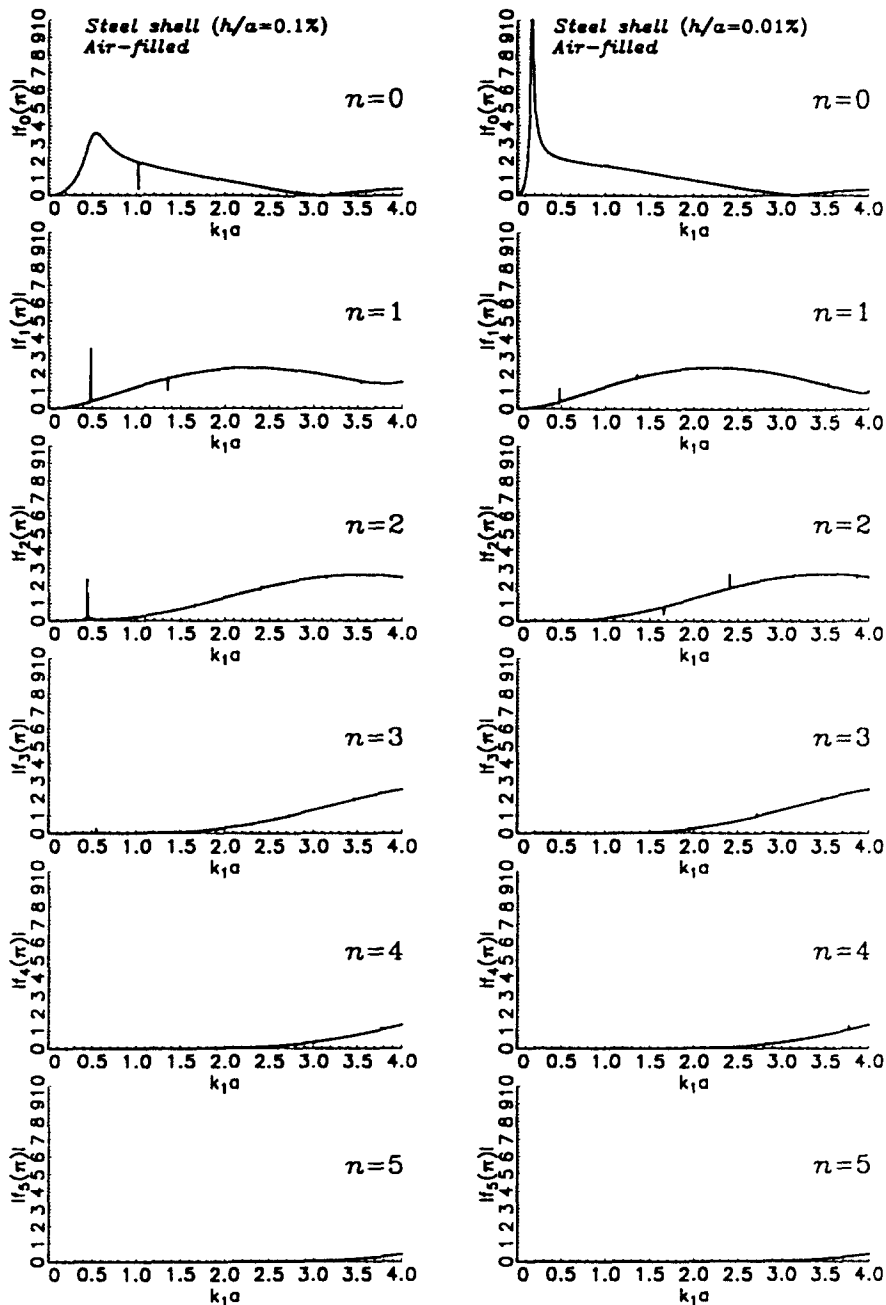
Fig. 3. The first few ($n = 0, 1, \ldots, 5$) partial waves contained within the backscattering cross-sections summed in the lower plots in Fig. 1. Relative shell thickness is 0.1% (0.01%) in the left (right) plots.

wave, because it can only be studied by a shell approach, whether exact (i.e. based on the three-dimensional theory of elasticity) or approximate (i.e. based on a shell theory). The 6×6 denominator determinant $D_n(x)$ in eqn (2) has zeros that are the (complex) eigenfrequencies of this fluid-loaded sound-excited shell. If the shell density ρ_2 is much larger than the water density ρ_1 (i.e. $\rho_2 \gg \rho_1$), and also much larger than the density of the filler fluid ρ_3 (i.e. $\rho_2 \gg \rho_3$), then the condition $D_n(x) = 0$ reduces to the vanishing of four possible 4×4 minor determinants D_{46}^{11}, D_{36}^{21}, D_{56}^{11} and D_{56}^{21}. The boundary conditions on $r = a, b$ that give rise to these determinants all imply that at least one shell surface is prevented from moving in the radial direction, except the vanishing of D_{56}^{21}. For this exception both shell surfaces are free from surface traction, and this is the condition required for the formation
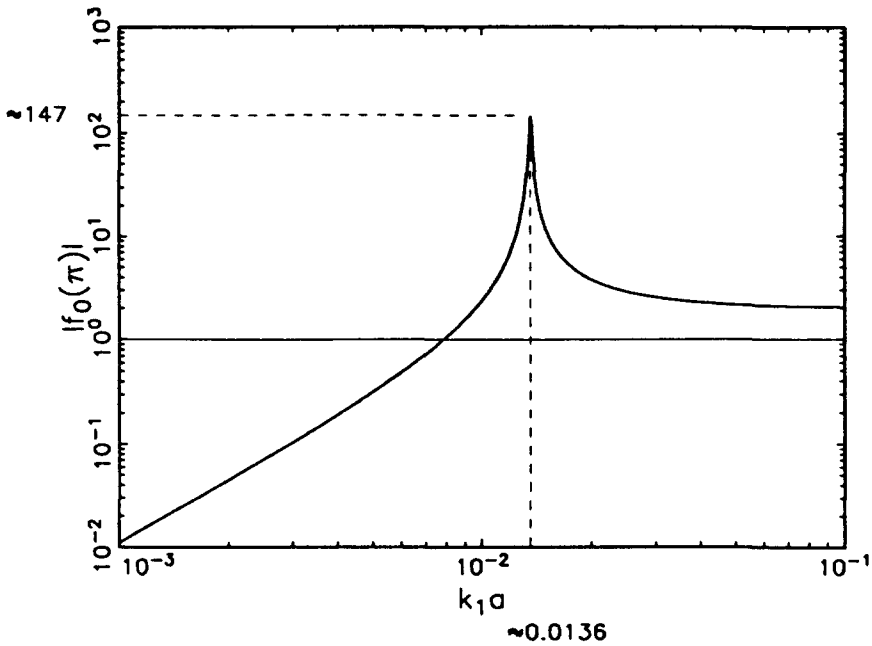
Fig. 4. The first partial wave, $|f_0(\pi, x)|$, contained within the backscattering cross-section of an air-bubble in water, which is the cause of the giant monopole resonance.

of proper Lamb waves. Therefore, the pertinent resonances of this shell in this frequency band appear as the roots of a generalized eigenfrequency condition for Lamb modes in submerged *shells*, obtained by Gaunaurd and Werby (1987). Ordinary lamb modes were originally studied for *plates in vacuum*, and we are now dealing with shells fluid-loaded on both surfaces with dissimilar fluids. The expanded version of that modified condition is

$$D_{56}^{21} = \begin{vmatrix} d_{12} & d_{13} & d_{14} & d_{15} \\ d_{32} & d_{33} & d_{34} & d_{35} \\ d_{42} & d_{43} & d_{44} & d_{45} \\ d_{62} & d_{63} & d_{64} & d_{65} \end{vmatrix} = 0, \tag{5}$$

which only has real roots x_{nl}, where n and l are the two indices required to label any root.

The families of roots of this equation are the *shell analogues* of the resonances usually associated with the symmetric (s_n) and antisymmetric (a_n) Lamb modes in plates, originally studied by Tolstoy and Usdin (1953, 1957). However, there are also additional roots of eqn (5). These extra roots—as well as the other ones—can be used to construct the dispersion plots for the phase velocities c_l^p of the circumferential waves travelling around the shell by means of the relation (Gaunaurd, 1989; Gaunaurd *et al.*, 1983):

$$\frac{c_l^p(x)}{c_1} = \frac{x_{nl}}{n + 1/2}, \tag{6}$$

where x_{nl} denotes the roots of eqn (5) corresponding to the lth surface wave.

Dispersion plots for the phase velocities, c_0^p, belonging to the a_0-branch in the frequency band: $0 \leqslant x \leqslant 20$ are displayed in Fig. 5 for a steel shell of various thicknesses (viz. $h/a = 1\%, 2.5\%, 5\%, \ldots$). The phase velocities associated with the s_0-waves are all greater than 5 km s^{-1}, and thus, they fall outside the upper bounds of Fig. 5. However, in the band: $1 \leqslant x \leqslant 2.3$, for a steel shell of relative thickness $h/a = 1\%$, there appears *another* branch of the dispersion curves also shown in the lower left corner of Fig. 5 for *another* permissible set of roots of eqn (5). It may be proper to call this branch the (Junger)
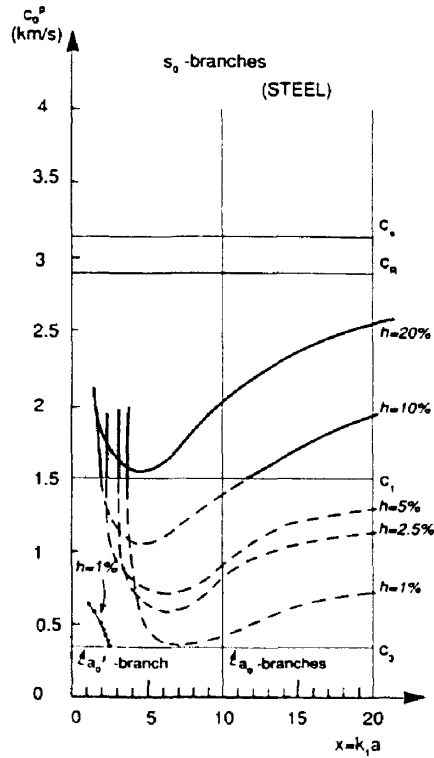
Fig. 5. Dispersion plot of the phase velocities of the zeroth order (a_0) antisymmetric Lamb wave versus $k_1 a$ for an air-filled spherical steel shell in water with relative shell thickness h/a = 1%, 2.5%, 5%, 10% and 20%. For the relative shell thickness of 1% the a_0^1-branch is displayed.

"a_0^1-branch". It seems to exist only within a (narrow) low-frequency band, where curvature effects are marked. We note that in contrast to ordinary dispersion plots for the a_0-branch, as obtained from *flat plate* approaches (Tolstoy and Usdin, 1953, 1957; Ayres *et al.*, 1987), the a_0-branch(es) shown in Fig. 5, obtained from the exact three-dimensional theory of elasticity contained in eqns (5) and (6) for fluid-loaded *shells*, exhibit values that grow — instead of decrease to zero —as x decreases. We further note that for subsonic phase velocities (viz. $c_0'' < c_1$, this corresponds to frequencies below the "coincidence" frequency), the a_0-branch is "turned-off" and thus, the corresponding curve is plotted in dashed lines in that region of Fig. 5. In that (subsonic) low-frequency region where the a_0 Lamb wave is still dormant, the s_0-wave (responsible for the s_0-branch of the phase velocity—not shown in Fig. 5) is "on" exerting its influence on the form-function, and so is the a_0^1-wave.

As stated before, the a_0^1-wave only exerts its influence in the band: $1 \leqslant x \leqslant 2.3$ (for h/a = 1%), and that is precisely the band where the large resonance features of the form-function are seen to occur in Figs 1 and 2. Finally, for an air-bubble in water there is no shell and no a_0^1-wave, but the dispersion curve that "corresponds" to the a_0-branch was studied earlier by Gaunaurd *et al.* (1983). In the high-frequency limit — which for a bubble is reached almost immediately, for $x \approx 1$ — the phase velocities of the interface waves approach the value of the speed of sound in *air* (Table 1, Fig. 5 and Fig. 1 in Junger, 1967).

6. CONCLUSIONS

We have studied, computed and displayed the large resonance features that are present at low frequencies in the form-functions of air-filled, spherical elastic shells in water. From the plots and the discussion it is obvious that these large features have a *multipole* character

and, for the thicknesses and materials shown, are caused by the superposition of the fundamental peaks of about half-a-dozen modes. As the shell thickness is made smaller (down to extremely and impractically small values) we note that: (i) fewer modes contribute to their formation; (ii) ultimately, as $b \rightarrow a$, only one mode (viz. the monopole mode, $n = 0$) contributes to it, just as in the air-bubble case; (iii) in that case the monopole resonance grows in amplitude from large to *giant*, and its spectral position shifts to lower values as low as $x \approx 0.0136$; (iv) the narrow, low-amplitude, overtones due to the presence of the air inside the shell remain present in the form-function and in the partial waves throughout the entire limiting process. Finally we have given a physical interpretation for the cause of this large resonance feature. It seems to be due to the additional zeros of eqn (5) that by means of eqn (6) produce an additional branch of the dispersion curves for the submerged shell. This branch is associated with a slow wave circumnavigating the shell at low frequencies. This branch seems to be analogous to a branch found earlier by Junger (1967) using a shell theory by Donnell (1933) to describe the shell motions. [For details of this theory, see for example Junger and Feit (1986).] We denoted this branch by a_0^1. For a spherical steel shell of relative thickness $h/a = 1\%$ this branch exists only for low frequencies (viz. for $1 \leqslant x \leqslant 2.3$). This is where the large and very noticeable resonance features of submerged shells actually appear. The slow wave with these values of its phase velocity is due to the shell curvature, and would have never emerged from a flat *plate* model of Lamb waves, whether in vacuum or fluid-loaded, as they have been studied before.

REFERENCES

Ayres, V. M., Gaunaurd, G. C., Tsui, C. Y. and Werby, M. F. (1987). The effects of Lamb waves on the sonar cross-sections of elastic spherical shells. *Int. J. Solids Structures* **23**, 937–946.

Brill, D. and Gaunaurd, G. C. (1987). Resonance theory of elastic waves ultrasonically scattered from an elastic sphere. *J. Acoust. Soc. Am.* **81**, 1–21.

Donnell, L. H. (1933). Stability of thin-walled tubes under tension. NACA Tech. Report No. 479, National Advisory Committee on Aeronautics, Washington, DC.

Gaunaurd, G. C. (1989). Elastic and acoustic resonance wave scattering. *Appl. Mech. Rev.* **42**, 143–192.

Gaunaurd, G., Scharnhorst, K. P. and Überall, H. (1979). Giant monopole resonances in the scattering of waves from gas-filled spherical cavities and bubbles. *J. Acoust. Soc. Am.* **65**, 573–594.

Gaunaurd, G. C., Tanglis, E., Überall, H. and Brill, D. (1983). Interior and exterior resonances in acoustic scattering: I.— Spherical targets. *Il Nuovo Cimento* **76B**, 153–175 (Fig. 1).

Gaunaurd, G. C. and Werby, M. F. (1987). Lamb and creeping waves around submerged spherical shells resonantly excited by sound scattering. *J. Acoust. Soc. Am.* **82**, 2021–2033.

Junger, M. C. (1967). Normal modes of submerged plates and shells. In *Fluid-Solid Interaction, Proc. ASME Symposium* (Edited by J. E. Greenspon) ASME, New York, pp. 79–119.

Junger, M. C. and Feit, D. (1986). *Sound, Structures, and Their Interaction*, 2nd Edn. MIT Press, Cambridge, MA.

Major, J. K. (Ed) (1969). *Physics of Sound in the Sea*, NAVMAT Publication #P-9675, Washington, DC; originally issued as: Summary Technical Report of Division 6, NDRC, Vol. 8 [Ch. 28, Fig. 1, p. 463], Washington, DC (1946).

Strifors, H. C. and Gaunaurd, G. C. (1989). Wave propagation in isotropic linear viscoelastic media. *J. Acoust. Soc. Am.* **85**, 995–1004.

Tolstoy, I. and Usdin, E. (1953). Dispersive properties of stratified elastic and liquid media: a ray theory. *Geophysics* **18**, 844–870.

Tolstoy, I. and Usdin, E. (1957). Wave propagation in elastic plates: low and high mode dispersion. *J. Acoust. Soc. Am.* **29**, 37–42.

APPENDIX

Five of the 28 non-vanishing elements, d_{ij}, listed in Ayres *et al.* (1987), Appendix, contain minor typographical errors that we wish to correct here to set the record straight. The underlined letter in each element is the typo:

$$d_{21} = k_1 a h_n^{(1)'}(k_1 a),$$

$$d_{41} = -4k_{d2} h y_n'(k_{d2}b) + [2n(n+1) - k_{t2}^2 b^2] y_n(k_{d2}b),$$

$$d_{44} = 2n(n+1)[k_{t2} b j_n'(k_{t2}b) - j_n(k_{t2}b)].$$

H. C. Strifors and G. C. Gaunaurd

$$d_{n4} = 2k_{12}bj'_n(k_{12}b) + [k^2_{12}b^2 - 2n(n-1) + 2]j_n(k_{12}b),$$

$$d_{n5} = 2k_{12}by'_n(k_{12}b) + [k^2_{12}b^2 - 2n(n-1) + 2]y_n(k_{12}b).$$

$y_n(\cdot)$ being the spherical Bessel function of the second kind of order n.

Furthermore, Fig. 2a in Ayres *et al.* (1987) refers to the large resonance feature in the cross-section displayed there, as the "monopole resonance". In view of the arguments discussed here, we now realize the *multipole* character of this feature.